

Changing the paradigm in f-containing cold molecules: the impact of spin-orbit coupling and f-d transitions on quasi-bound vibrational states.

Marta Gałyńska,¹ Matheus M. F. de Moraes,^{1, a)} Paweł Tecmer,^{1, b)} and Katharina Boguslawski^{1, c)}
*Institute of Physics, Faculty of Physics, Astronomy, and Informatics, Nicolaus Copernicus University in Toruń,
Grudziadzka 5, 87-100 Toruń, Poland*

(Dated: 25 July 2024)

Present-day state-of-the-art ab initio many-body calculations on f-block containing cold molecules heavily focus on perturbative approaches for spin-orbit coupling and exclude a substantial part of the atomic transitions in the f - and d -shell. Here, we demonstrate the cruciality of a proper relativistic treatment of the f - and d -shell in Yb-containing diatomics and the inclusion of $f \rightarrow d$ transitions to obtain physically sound elastic scatterings and pre-dissociation lifetimes. We focus on state-of-the-art relativistic many-body calculations for the Yb atom's ground- and excited-state and the YbLi⁺ potential energy surface. For that purpose, we exploit various quantum many-body methods, namely a spin-free and four-component implementation of the coupled cluster singles and doubles (CCSD) model and its equation of motion extensions, spin-free complete active space self-consistent field, and internally contracted multi-reference (MR) configuration interaction approaches, and spin-free MRCCSD with a perturbative and full triples correction. We oppose scalar relativistic calculations to four-component variants to support the reliability of our EOM-CCSD study and shed new light on the interplay between these systems' spin-orbit coupling and the proper treatment of relativistic effects. Most importantly, we observe a significant shift in the electronic spectra of the $f \rightarrow d$ excitation block. We also provide new reference potential energy surfaces for ground and excited states for which theoretically sound elastic scattering and pre-dissociation lifetimes are calculated.

I. INTRODUCTION

The recent discovery of laser cooling¹ rendered experimental investigations on compounds in their electronic ground state at temperatures close to absolute zero possible. During the last two decades, many sophisticated experimental methods such as helium buffer gas cooling,² photoassociation,³ and magnetic Feshbach resonances⁴ were extensively applied to explore the chemistry and physics of so-called cold and ultracold atoms and molecules, which are typically studied in the range of 1.0 K and 1.0 mK, respectively. These experiments facilitate measurements of atoms or molecules with remarkable precision by controlling their specific quantum state. Quantum many-body methods,⁵⁻⁷ on the other hand, can predict all fundamental properties associated with the ground and lowest-lying excited states of atoms and molecules at absolute zero temperature. Thus, cold and ultracold chemistry can combine theory and experiment to discover fundamental properties of matter in the quantum realm.

However, experiments on cold and ultracold molecules are not trivial. Problematic or difficult experimental techniques are, for example, laser cooling for molecular systems (due to their complex hyperfine structure arising from the interaction between the magnetic and electric field of the nuclei and electrons as well as their rovibronic coupling) and evaporative cooling (due to the large probability of three-body loss collisions). At the same time,

temperatures close to absolute zero are fairly suitable for quantum mechanical simulations as the thermal motion is minimized and the systems are predominantly in their ground state configurations. Highly accurate quantum many-body calculations can provide much sought-after local properties of cold molecules. Examples are bond lengths,^{8,9} scattering constants,^{10,11} electric dipole moments,¹² electronic and vibrational spectra,¹³⁻¹⁶ which on their part provide fundamental insights on the interaction of atoms and molecules.^{17,18} Furthermore, theoretical data on cold molecules is of the utmost importance in experimental studies to, for instance, parameterize experimental setups, define starting points for laser-induced methods, and interpret or validate experimental results.

In the early days, the cold chemistry community focused on alkali atoms because of their simple hydrogen-like structure and alkali metal diatomic systems. Thereafter, ytterbium-based molecules became highly valuable. Ytterbium's closed f-shell and the $4f^{14}6s^2$ ground-state electronic configuration make the electronic structure of the ytterbium atom similar to the group-II atoms. The simplest example is the YbLi⁺ system. Tomza *et al.*¹² conducted a theoretical study on YbLi⁺ focusing on the Yb⁺ and Li atoms as precursors. That study obtained and analyzed four singlet and five triplet states. The closed-shell nature of the system allowed for ground-state computations using the canonical coupled-cluster singles and doubles and perturbative treatment of triple excitations (CCSD(T)) from the equilibrium region up to the dissociation limit. Excited states were modeled using the CCSD(T) and equation of motion coupled cluster singles and doubles with perturbative triples (EOM-CC3) methods. Although the investigated electronic spectrum of YbLi⁺ covers the range of 25000–35000 cm⁻¹ at the equi-

^{a)}Electronic mail: matheusmorat@gmail.com

^{b)}Electronic mail: ptecmer@fizyka.umk.pl

^{c)}Electronic mail: k.boguslawski@fizyka.umk.pl

librium and dissociation regions, respectively, no state correlated to the $\text{Yb}(4f^{13}5d6s^2)$ electronic configuration was reported. Studies on similar diatomic ytterbium-containing molecules suggest that there is more than one state to consider (other than f^{14}) and that these states' position strongly depends on the degree of correlation included.^{19,20} Very recently, Pototschnig *et al.*¹⁶ showed for YbF that some $\text{Yb}^+(4f^{13}6s)$ correlated states have T_e values around 5000 cm^{-1} and effectively cross the ground state correlated with the $\text{Yb}^+(4f^{14}6s)$ electronic configuration. Therefore, these states must be considered in quantum many-body calculations to avoid potentially non-negligible effects on the ground and low-lying states of YbLi^+ . Unfortunately, standard multi-reference methods, like the complete active space self-consistent field²¹ (CASSCF) theory or the multi-reference configuration interaction (MRCI) approach, are not flexible enough to cope with many open-shell $4f$, $6s$, $6p$, and $6d$ configurations on an equal footing.

Closed-shell electronic structures, like YbLi^+ , are difficult to cool and trap experimentally. Consequently, the experimental focus has been shifted towards open-shell doublet and triplet state molecules. The YbX ($X = \text{Li}, \text{Na}, \text{K}, \text{and Rb}$) doublet ground-state series is a well-known example.^{10,13,14,22,23} Similar to the closed-shell YbLi^+ molecule, theoretical calculations for YbLi un-veiled low-lying states correlated with the $\text{Yb}(4f^{13}5d6s^2)$ electronic configuration. Considering the possible presence of both f^{13} and f^{14} configurations of Ytterbium, reliable theoretical studies have to provide a balanced description of both electronic configurations.

Lu and Peterson²⁴ showed for a lanthanide series that the spin-orbit coupling (SOC) effect on the ionization potentials from the $6s$ and $5d$ shell are substantially smaller than removing an electron from the $4f$ -shell. Specifically, for the $4f$ -shell ionization ($\text{Yb}^{2+}(4f^{14}) \rightarrow \text{Yb}^{3+}(4f^{13})$) the SOC value increases to $4\,400\text{ cm}^{-1}$. Therefore, a reliable theoretical picture of the ionized and excited-state electronic structures must first correctly model all configurations relevant to the problem. This includes, but is not restricted to, $4f$ excitations. Then, SOC has to be included as it can drastically alter the relative energy among states.²⁵

This work aims to remedy this problem by providing a balanced treatment of relativistic and electronic correlation effects for the ground and excited-state electronic structures of YbLi^+ by using the four-component (4C) Dirac–Coulomb Hamiltonian and various coupled-cluster methods. Our study shed new light on the electronic structures and spectroscopic characterization of the Yb atom and the YbLi^+ molecule, providing a new reference point for experimental manipulations.

II. COMPUTATIONAL DETAILS

A. 4C relativistic calculations

The all-electron relativistic calculations were done using the 4C Dirac–Coulomb Hamiltonian, in which the $(SS|SS)$ integrals were approximated by a point charge model,²⁶ in the `Dirac19` software package.²⁷ All computations utilized the all-electron `dyall.v3z` basis sets.^{28,29} The ground-state electronic calculations were computed with the relativistic version of the CCSD(T) method.^{30,31} The low-lying excited states of the closed-shell Yb atom and the YbLi^+ molecule were investigated using the relativistic version of the equation of motion coupled cluster singles and doubles (EOM-CCSD) method.³² For the Yb atom, we correlated spinors in the energy range of $[-2; 100\,000] E_h$. For the YbLi^+ molecule, spinors in the energy range of $[-4; 100] E_h$ were correlated in the CC calculations. That corresponds to 12 occupied and 253 virtual spinors in the Yb atom, and 13 occupied and 203 virtual spinors in the YbLi^+ molecule. Among others, these include the occupied $\text{Yb}:5p$, $\text{Yb}:4f$, and $\text{Yb}:6s$, and virtual $\text{Li}:2s$, $\text{Li}:2p$, $\text{Li}:3s$, $\text{Yb}:6p$, $\text{Yb}:5d$, $\text{Yb}:7s$, and $\text{Yb}:6d$ orbitals.

B. Spin-free and perturbative spin-orbit calculations

The spin-free CCSD(T) and EOM-CCSD calculations were performed with the spin-free Dyal Hamiltonian³³ and the same computational setup as described in subsection II A.

Internally contracted multireference configuration interaction³⁴ (MRCI) calculations with the Davidson correction³⁵ (MRCI+Q) were performed using the `Molpro2019` software package.^{36,37} Internally contracted multi-reference coupled cluster (MRCCSD, MRCCSD(T), and MRCCSDT) calculations were carried out in the *General Contracted Code* (GeCCo) software package.^{38,39} The all-electron `cc-pVnZ-DK3` ($n=\text{T}, \text{Q}$) basis set²⁴ was utilized for Yb and `cc-pVnZ-DK` ($n=\text{T}, \text{Q}$) basis sets⁴⁰ was employed for the Li atom. The scalar relativistic effects were accounted for using the third-order Douglas–Kroll–Hess (DKH3) approach.^{41–46}

All multireference calculations used Restricted Active Space (RAS) orbitals to generate the reference wave function. The active space is composed of 17 electrons distributed in 16 orbitals, $\text{RAS}(17,16)$, and covers $\text{Yb}:4f$, $\text{Yb}:5d$, and $\text{Yb}:6s$, $\text{Li}:2s$, and $\text{Li}:2p$ orbitals. All calculations used the C_{2v} Abelian point group symmetry. Specifically, the active space contains six orbitals in symmetry A_1 , four in B_1/B_2 , and two in A_2 , denoted as $(6,4,4,2)$. In the restricted orbital occupation calculations, the active space was divided into $\text{RAS1}(2,2,2,1)$ and $\text{RAS2}(4,2,2,1)$, containing the $\text{Yb}:4f$ -shell, and the remaining inner-valence orbitals, respectively. Two sets of calculations were carried out to obtain the occupation-specific $4f^{13}$ and $4f^{14}$ states. The molecular orbitals were

optimized in a state-average fashion. For the occupation-specific $4f^{14}$ set of calculations, 43 states were averaged, including 22 A_1 , 12 B_1/B_2 , and 9 A_2 states. For the $4f^{13}$ set, 41 states were considered: 15 A_1 , 14 B_1/B_2 , and 12 A_2 states.

A similar procedure to YbLi^+ was employed for multireference calculations on Yb and Yb^+ . The $4f^{14}$ active space included RAS2(4,2,2,1), encompassing $\text{Yb}:6s$, $\text{Yb}:6p$, and $\text{Yb}:5d$ orbitals. For the $4f^{13}$ states, the RAS1(2,2,2,1) active space was used, comprising $\text{Yb}:4f$ orbitals and RAS2(4,2,2,1) comprising $\text{Yb}:6s$, $\text{Yb}:6p$, and $\text{Yb}:5d$ orbitals. The core-valence correlation was also considered for the $\text{Yb}:5s$ and $\text{Yb}:5p$ orbitals.

The SOC was included perturbatively on top of spin-free energies by diagonalizing the matrix of electronic and spin-orbit operators. Using the one- and two-electron Breit–Pauli operators⁴⁷ in the basis of the spin-free eigenstates ($\Lambda+S$) electronic of the Breit–Pauli Hamiltonian.

C. Vibrational analysis

We used the QuAC software⁴⁸ to perform a rovibrational and scattering analysis of the computed PESs. Rovibrational parameters were obtained by numerical integration of the radial Schrödinger equation

$$\left[\frac{\partial^2}{\partial r^2} - \frac{J(J+1)}{r^2} + V(r) - E_{v,J} \right] \chi_{v,J} = 0, \quad (1)$$

where J ($J \in \mathbb{N}$) is the rotational quantum number and $V(r)$ is the fitted electronic potential using a cubic spline expansion. The resulting rovibrational levels were then fitted to obtain the Dunham parameters,⁴⁹

$$E(v, J) = \omega_e(v + 1/2) - \omega_e x_e (v + 1/2)^2 + B_e J(J + 1). \quad (2)$$

In the above equation, ω_e is the vibrational constant, $\omega_e x_e$ accounts for the anharmonicity in the vibrational energy levels, and B_e denotes the rotational constant. The phase-shift parameter $\eta_J(E)$ has been computed via the method of partial waves.⁵⁰ The derivative of the phase-shift with respect with the collisional energy has used to compute numerically the collisional time-delay $\tau_J(E)$ via the five-point method.⁵¹

III. RESULTS

A. Yb atom

We will start with the assessment of our theoretical models in describing the electronic structures of the closed-shell Yb and open-shell Yb^+ atoms and their spectra. We will compare our results against the experimental data presented in Refs. 52,53. Specifically, we exploit various levels of relativistic Hamiltonians and electronic

structures methods. Our results are collected in Table I. The electronic excitations can be further divided into $4f^{14}$ or $4f^{13}$ states. We should stress that the computed SO splittings agree with the experimental data, irrespective of the chosen configuration ($4f^{14}$ or $4f^{13}$) and methodology (perturbative SOC or 4c Hamiltonian). On the other hand, the accuracy of the relative energies widely varies with the employed methodology and the state’s configuration.

The first excited state of the Yb atom is the f^{14} state ${}^3P_u(6s \rightarrow 6p)$, where the electron is excited from the Yb 1S_g ground state, followed by the ${}^3D_g(6s \rightarrow 5d)$ state, which split into three Ω states.⁵⁴ These low-lying f^{14} states (3P_u and 3D_g) as well as the first ionization potential (2S_g) calculated using 4c SOC-EOM-CCSD are similar to the SOC-MRCISD+Q results. Furthermore, 4c SOC-EOM-CCSD almost exactly reproduces the experimental values (differences are between 200 and 1200 cm^{-1}). The error for the ionization potential of the Yb^+ $f^{13}6s^2$ state reduces with the level of theory according to SS-RASSCF > MRCISD > MRCISD+Q > MRCCSD > EOM-CCSD \approx MRCCSD(T) \approx MRCCSDT (with errors of -35 000, -13 000, -9 000, -6 500 and -4 000 cm^{-1}). The SS-RASSCF error highlights that dynamic correlation considerably differs in the $4f^{14}$ and the $4f^{13}$ states. Such a gap in the correlation energy is similar to the one reported for the third and fourth ionization potentials.²⁵ Thus, the main factor for this gap emerges from the change in the number of the $4f$ electrons and not in the system’s charge. The similar performance of MRCCSD(T) and MRCCSDT supports this case. Hence, we can conclude that the $4f^{14}$ correlations are crucial and need to be properly accounted for by including either higher excitations or sufficiently large virtual spaces. Finally, the difference in error between MRCCSD and EOM-CCSD gives us an estimate of the error caused by the lack of orbital relaxation in the reference of the latter, which is around 2 500 cm^{-1} .

For the neutral atom, the targeted f^{13} states include the excitations from the Yb $4f$ to the $5d$ shell, resulting in the Yb $4f^{13}6s^25d$ configuration. For these f^{13} states, the 4c SOC-EOM-CCSD errors in the Yb $4f$ to $5d$ excitations increase to approximately -6 000 and -8 000 cm^{-1} compared to the f^{14} states. Similarly, the error of the MRCISD+Q results increases to around 5 000 cm^{-1} . We should stress that the error decreases to below 2 000 cm^{-1} without the Davidson correction. This behavior indicates a cancellation of errors at the MRCISD level. Most likely, the error from the $4f^{13}-5d^1$ interaction cancels out the one from the $4f^{14}$ shell at the MRCISD level, while the lack of orbital relaxation leads to a higher absolute error in EOM-CCSD calculations.

Consequently, the relative errors in (excitation and ionization) energies compared to the experimental value appear to primarily originate from the missing $4f^{14}$ correlation energy, either due to the lack of higher excitations or the limited virtual space. This difficulty might be directly transferable to ytterbium-containing molecules.

TABLE I. The excitation energies and ionization potentials of the Yb atom calculated with wave function-based methods including icMRCISD, icMRCISD+Q, and 4c EOM-CCSD. The experimental values are obtained from Ref. 52.

Main config.	Term	J	MRCISD	MRCISD+Q	4c EOM-CCSD	Exp. 52
Excitation energies						
$4f^{14}6s6p$	3P_u	0	15 349	16 186	17 091	17 288
		1	16 103	16 932	17 800	17 992
		2	18 054	18 891	19 567	19 710
$4f^{14}6s5d$	3D_g	1	25 487	25 319	25 659	24 489
		2	25 756	25 595	25 881	24 751
		3	26 263	26 095	26 271	25 270
$4f^{14}6s6p$	1P_u	1	26 685	26 931	26 159	25 068
		2	24 134	28 928	15 601	23 188
$4f^{13}5d6s^2$	$(\frac{7}{2}, \frac{3}{2})_u$	5	26 661	31 502	19 124	25 859
		3	28 202	33 035	21 043	27 445
		4	29 012	33 786	22 012	28 184
		6	28 285	33 173	20 500	27 315
$4f^{13}5d6s^2$	$(\frac{7}{2}, \frac{5}{2})_u$	2	29 288	34 038	21 701	28 196
		1	31 181	35 978	20 911	28 857
		4	30 957	35 701	23 699	29 775
		3	31 310	36 107	24 136	30 207
		5	31 693	36 493	24 565	30 525
$4f^{13}5d6s^2$	$(\frac{5}{2}, \frac{5}{2})_u$	0	35 698	40 481	27 518	n/a
		1	39 079	43 951	31 676	n/a
		5	39 373	44 207	32 023	n/a
		2	40 249	45 064	33 082	n/a
		3	41 520	46 301	34 549	n/a
$4f^{13}5d6s^2$	$(\frac{5}{2}, \frac{3}{2})_u$	4	42 017	46 775	35 167	n/a
		4	36 780	41 640	29 542	n/a
		2	37 894	42 645	30 802	n/a
		1	39 259	44 451	34 590	n/a
$4f^{14}6s5d$	1D_g	3	40 136	44 918	33 653	n/a
		2	28 424	28 795	28 259	27 678
Ionization potentials						
$4f^{14}6s$	2S_g	1/2	47 944	48 791	50 478	50 443
$4f^{13}6s^2$	2F_u	7/2	58 882	63 157	67 600	71 862
		5/2	69 206	73 481	78 252	82 011

Therefore, we should be aware of a similar underestimation in relative energies among states correlated to these $4f^{13}$ configurations in the YbLi^+ cation.

B. YbLi^+ Electronic Structure

Since the neutral ytterbium and lithium atoms feature similar ionization potentials, the excited states of YbLi^+ can be attributed to two different configurations, namely $\text{Yb}+\text{Li}^+$ and Yb^++Li .

We start our discussion with multi-reference methods commonly used to model excited-state structures of diatomics. As observed for the isolated atom, the lack of dynamic correlation in the reference wave function leads SS-RASSCF to underestimate the energies of the $4f^{14}$ states compared to the $4f^{13}$ ones. However, it is computationally infeasible to (partly) recover the dynamic correlation energy via MRCISD considering the full inner-valence with $4f^{13}$ configurations along the full PES. Therefore, we calculated only single points with

smaller wave function expansions to estimate the vertical singlet excitation energies of A_1 symmetry. Without the inclusion of core-valence correlation and employing a minimal active space ($4f$ -shell, σ and σ^*), the low-lying $4f \rightarrow \sigma^*$ states are around 24 000 and 20 500 cm^{-1} for MRCISD with and without the Davidson correction, respectively. Including the full $5d$ shell in the active space shifts the vertical MRCISD transition with mainly $4f \rightarrow \sigma^*$ character to around 37 500 cm^{-1} . Adding a Davidson correction lowers them to 19 000 cm^{-1} . Likewise, MRCISD states featuring $4f \rightarrow 5d$ excitations are raised to a range between 35 000 to 40 000 cm^{-1} , which are further increased by the Q correction (between 40 000 to 50 000 cm^{-1}). Such a large energy variation indicates an insufficient reference state in the multi-reference treatment. Therefore, the best estimate from multi-reference methods is a small density of $4f^{13}$ -type states in the range of 20 000 to 25 000 cm^{-1} , followed by a more dense region above 30 000 cm^{-1} .

As in the atomic case, EOM-CCSD allows us to target multiple distinct excitations with satisfying accuracy and

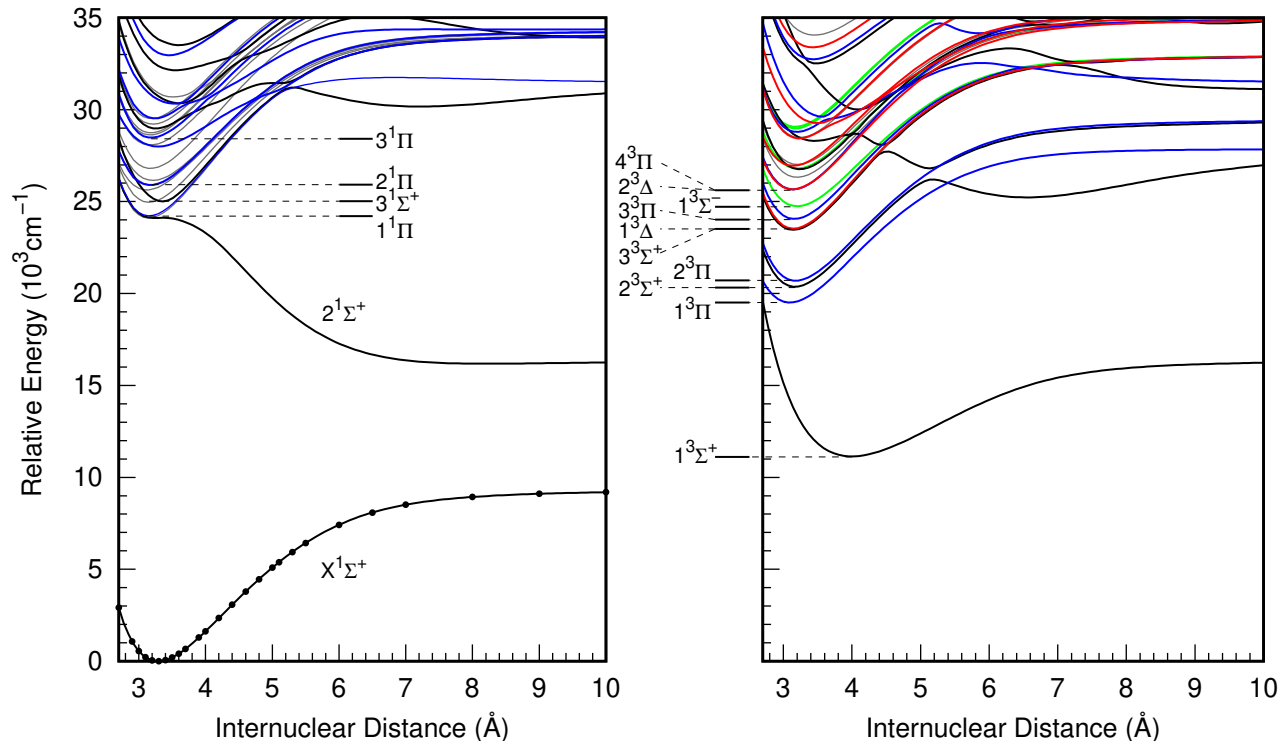


FIG. 1. Low-lying excited singlet (left panel) and triplet (right panel) states of YbLi^+ calculated with spin-free EOM-CCSD/VTZ method. States that are able to span $\Omega = 0^+$ or 1 are colored. Symmetry Σ^+ in black, Σ^- in green, Π in blue and Δ in red. Other states are plotted in gray. States with minima up to around 26 000 cm^{-1} are labeled. For all calculated data points sorted per spatial and spin symmetries see SI.

relatively low computational cost. The spin-free ($\Lambda+S$) PESs are shown in Figure 1. States dominantly composed of $4f^{14}$ configurations agree with the ones found in the literature,¹² namely, $X^1\Sigma^+$, $2^1\Sigma^+$, $1^3\Sigma^+$ and $1^3\Pi$. Including states mainly composed of $4f^{13}$ configurations drastically increases the density of states between 20 000 and 30 000 cm^{-1} , which qualitatively agrees with the multi-reference estimate. This region covers the $3^3\Sigma^+$ state which directly interacts with the $2^1\Sigma^+$ state (note the avoided crossing around 3.5 Å) and the $1^1\Pi$, $2^3\Sigma^+$, and $2^3\Pi$ ones.

Although the inclusion of states with $4f^{13}$ character may modify the excited-state structure of the YbLi^+ cation at the spin-free level, these states are high in energy compared to the second dissociation channel (i.e. $\text{Yb}^+(^2S_g)+\text{Li}(^2S_g)$). Therefore, all spin-free states of interest for a low energy collision of Yb^++Li are mainly composed of $4f^{14}$ configurations. As already observed for the isolated ytterbium atom, SOC has, however, a large effect over the states of $4f^{13}$ character, in particular, when compared to the $4f^{14}$ counterpart. Figure 2 demonstrates this change in relative energies caused by SOC deduced from the 4c EOM-CCSD results. The PESs with minima below 21 000 cm^{-1} are labeled based on the spin-free calculation to simplify the visualization and discussion and their spectroscopic constants are summarized in Table II. Note, however, that the SOC states feature

large mixing of spin-free configurations, in particular for $1^3\Pi_1$, $2^3\Sigma_1^+$, and $2^3\Pi_1$, which comprise, among others, excitations from Yb $4f$ to Li $2s$, Yb $4f$ to Yb $7s$, Yb $4f$ to Yb $5d$, and Yb $6s$ to Yb $6p$.

Most importantly, the inclusion of SOC shrinks the relative energy gap leading to qualitative changes in the curves associated with the second dissociation channel and allowing the non-relativistic spin-forbidden triplet-singlet radioactive transitions. These changes affect the Yb^++Li collision process. First, the $\Omega = 1$ state spanned by the $1^3\Sigma^+$ spin-free state mixes with the $1^3\Pi$ at small internuclear distances. The second state of $\Omega = 0^+$ symmetry suffers a much larger qualitative change, with an avoided crossing around 4.5 Å. This change in wave function character creates a meta-stable state with a relatively small potential barrier that can also affect the radiative decay of the system.

To estimate the effects of SOC and $4f^{13}$ configurations on the light emission processes of the excited YbLi^+ cation, we calculate the transition dipole moments (TDMs) using the perturbative SO-RAS split with the SF-EOM-CCSD total energies as the unperturbed energies. Figure 3 summarizes the TDMs with values larger than 0.5 D, between the ground state and states whose minima are lower than 22 000 cm^{-1} . The adiabatic transition dipole values to the spin-allowed $2^1\Sigma^+$ state (dashed line with hollow marks) agrees with the

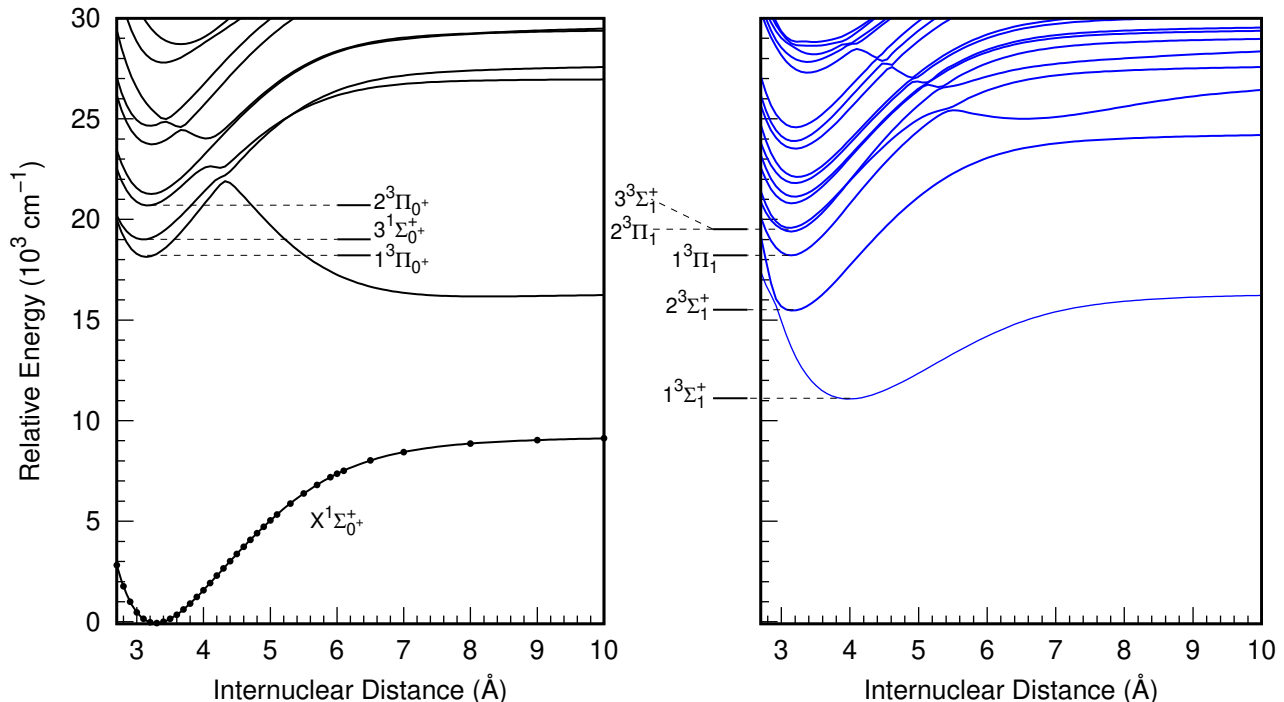


FIG. 2. Low-lying $\Omega = 0^+$ (in black; left panel) and $\Omega = 1$ (in blue; right panel) states of YbLi^+ calculated with spin-orbit-coupling EOM-CCSD/VTZ. The state labelling has been attributed based on the spin-free calculation (Figure 1). For all calculated data points sorted per Ω value see SI.

non-relativistic results found in the literature.¹² On the other hand, the diabatic curve substantially reduces the transition in the equilibrium distance (between 2.5 and 4.0 Å), caused by the avoided crossing with the spin-forbidden $1^3\Pi_{0^+}$ state. However, the large SOC leads to non-negligible values in TDM. Similarly, substantial TDMs are obtained for $X^1\Sigma_{0^+}^+ - 2^3\Pi_1^+$ and $X^1\Sigma_{0^+}^+ - 1^3\Sigma_1^+$, both coupled to the non-relativistic spin-forbidden transitions.

The presence of a meta-stable (or quasi-bound) state with a non-negligible TDM to the ground state allows for an additional route via tunnelling followed by a radiative decay. Three resonance states are likely to be reached from tunneling through collisions, as shown via the phase shift (η_J) for $J = 0$ in Figure 4(a). These resonances can be correlate with the vibrational levels of the meta-stable state ranging from $v=13$ to $v=15$, listed in Table III. The pre-dissociation lifetime of these meta-stable vibrational states can be calculated by the collision delay time (Figure 4(b)) at the resonance energies divided by a factor of four.⁵⁵ The pre-dissociation lifetime, in particular for $v=14$ (0.127 ns), is comparable to the partial radiative lifetime of this state (2.472 ns). Therefore, the tunneling route is viable and could be enhanced by stimulated emission. The main populated vibrational levels of the ground states should be $v=10, 11$, and 12 , which have larger Einstein coefficients with respect to the accessible meta-stable vibrational state. Considering misaligned collisions, that is, for $J > 0$, the range

of resonance energies extends from around 5 000 up to 6 000 cm^{-1} . Within this collision energy range between 5 000 and 5 400 cm^{-1} , the pre-dissociation lifetimes are above 10^{-10}s .

As discussed before, it is likely that the gap between the $4f^{14}$ and $4f^{13}$ -type states may be underestimated in the 4c EOM-CCSD method, that is, they represent a lower limit. An upper limit can be calculated within MR-CISD+Q using only $4f^{14}$ states, which is analogous to excluding any coupling between $4f^{14}$ and $4f^{13}$ states. Without the presence of $4f^{13}$ configurations, the $1^3\Pi_{0^+}$ has a higher excitation energy ($T_e=18999 \text{ cm}^{-1}$) and lower dissociation energy ($D_e=-2823 \text{ cm}^{-1}$), but a similar barrier of 5 698 cm^{-1} . As a consequence, the collisional energy required to access quasi-bound rovibrational states is not altered by the lack of $4f^{13}$ configuration, but the accessible levels are $v = 12$ and 13 .

Additionally, with the smaller mixing among configurations the TDM is substantially reduced in the equilibrium distance (compare black and gray curves from Figure 3). As a consequence, the partial radiative life-time of the accessible state increases slightly, namely, 37 and 27 ns for $v = 11$ and 12 , respectively. The former decays mainly to the $v = 8$ ground state, while the latter decays to $v = 9$, as the PESs minima are shifted from each other. Therefore, although the presence of $4f^{13}$ configurations enhances the inelastic formation of YbLi^+ ground state molecules, if the excited state is composed of only $4f^{14}$ configurations, the tunneling route allowed via SOC

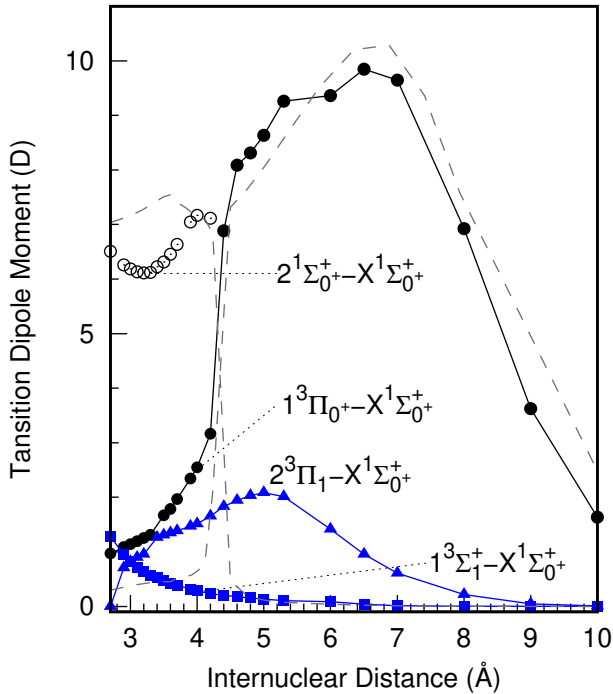


FIG. 3. Transition dipole moment in Debye (D) calculated between the $X^1\Sigma_0^+$ ground state and three Ω states: $1^3\Sigma_1^+$ (filled circle), $2^3\Pi_1^+$ (filled triangle), $1^3\Pi_0^+$ (filled square) and one following the $2^1\Sigma_0^+$ adiabatically (hollow circles). Values obtained using the perturbative SO-RASCI approach with unperturbed SF-EOM-CCSD energies. Dashed gray lines marks the $2^1\Sigma_0^+ - X^1\Sigma_0^+$ and $1^3\Pi_0^+ - X^1\Sigma_0^+$ transition dipole moment using $4f^{14}$ -configuration MRCISD+Q unperturbed energies.

TABLE II. Spectroscopic parameters including equilibrium bond length (r_e), intermolecular distance of ro-vibrational ground state (r_0), minimum electronic energy (T_e), vibrational constant – first term (ω_e), vibrational constant – second term ($\omega_e x_e$), rotational constant in equilibrium position (B_e), electronic dissociation energy (D_0), zero-point dissociation energy (D_e) calculated for the Ω states of $^{174}\text{Yb}^7\text{Li}^+$. The r_e and r_0 are given in Angstrom (\AA), while other quantities are given in wave number (cm^{-1}).

State	$r_e(r_0)$	T_e	ω_e	$\omega_e x_e$	B_e	$D_e(D_0)$
$X^1\Sigma_0^+$	3.285(3.285)	0	231.13	1.38	0.232	9183(9068)
$1^3\Sigma_1^+$	3.986(4.663)	11 141	148.28	0.85	1.149	5150(4992)
$2^3\Sigma_1^+$	3.168(3.220)	15 531	260.10	1.00	0.241	8728(8602)
$1^3\Pi_0^+$	3.139(3.124)	18 203	259.30	1.64	0.256	-1897(-2027)
$1^3\Pi_1$	3.140(3.155)	18 278	259.66	1.71	0.251	8222(8093)

[†]Disregarding the repulsive region between 4.3 and 10 \AA .

remains likely to be observe experimentally.

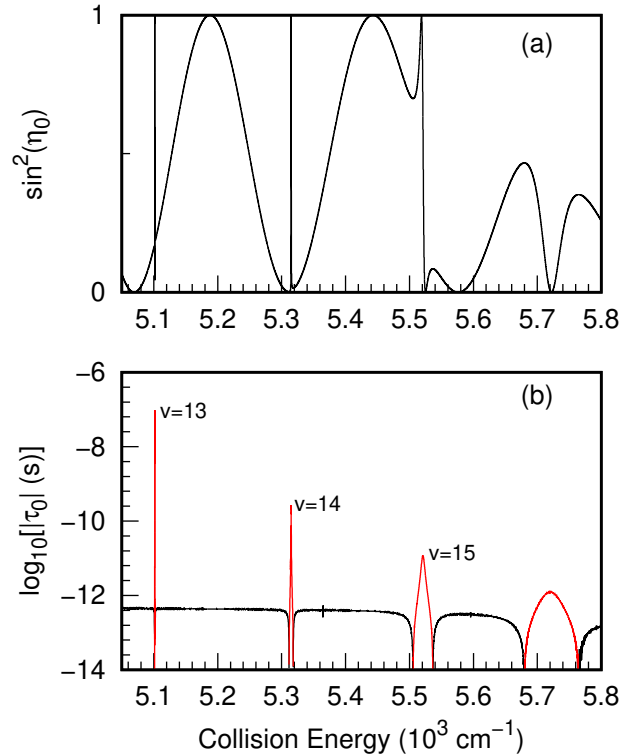


FIG. 4. Elastic scattering results for state $1^3\Pi_0^+$ shown in Figure 2 of the $^{174}\text{Yb}^7\text{Li}$ system. (a) sine square of the phase shift η_J , for $J = 0$. (b) Logarithm of the absolute values of the collisional time-delay, τ_J , for $J = 0$. In red positive values of τ_0 and in black negative ones. The labels mark the corresponding quasi-bound vibrational states.

TABLE III. Vibrational energy levels (in cm^{-1}) for $X^1\Sigma_0^+$ and $1^3\Pi_0^+$ states shown in Figure 2.

v	$^{174}\text{Yb}^7\text{Li}$		$^{174}\text{Yb}^6\text{Li}$	
	$X^1\Sigma_0^+$	$1^3\Pi_0^+$	$X^1\Sigma_0^+$	$1^3\Pi_0^+$
0	115	130	124	140
1	343	386	369	415
2	569	639	612	687
3	791	889	851	956
4	1012	1135	1087	1219
5	1229	1377	1320	1479
6	1443	1616	1550	1734
7	1655	1851	1776	1986
8	1865	2084	2000	2234
9	2071	2314	2221	2480
10	2276	2541	2439	2723
11	2477	2766	2654	2962
12	2676	2987	2865	3196
13	2872	3205	3073	3426
14	3065	3418	3276	3644
15	3255	3622	3476	—

[†]Disregarding the repulsive region between 4.3 and 10 \AA .

IV. CONCLUSIONS

This work provides a fully relativistic *ab initio* picture of the ground- and excited-state of Yb, Yb⁺ and YbLi⁺ based on the 4c Dirac–Coulomb Hamiltonian and the EOM-CCSD approach. For the first time, we report a complete electronic spectrum of the Yb atom, which includes all possible single $4f \rightarrow 5d$ electronic transitions. Our theoretical data agrees very well with the NIST reference atomic levels in the lower part of the spectrum and complements the missing $4f \rightarrow 5d$ block of 10 transitions in the Yb spectrum. Due to the incompleteness of the available basis sets and the limited amount of orbital relaxation effects in our theoretical model, the agreement with the experimental Yb spectra of the $4f \rightarrow 5d$ block is less satisfactory.

Nonetheless, we show that the impact of the $4f \rightarrow 5d$ excitations on the electronic spectra of YbLi⁺ is nonnegligible, especially when spin-orbit coupling is accounted for from the beginning in the 4c formalism, which results in the lowering of the $4f \rightarrow 5d$ block of transitions by a few thousand cm⁻¹. That, in turn, affects the resulting YbLi⁺ spectroscopic characterization. Specifically, we observe that:

- the second $\Omega = 0^+$ state is no longer repulsive and forms a meta-stable state
- that meta-stable state leads to quasi-bound rovibrational levels that are accessible via tunneling
- the presence of $f^{14}-f^{13}$ interactions increase the transition dipole moment and, as a consequence, the probability of radiative-decay to the ground-state of YbLi⁺.

In conclusion, our results suggest that higher collision energies (above 5 000 cm⁻¹) should be used in experimental studies to increase the formation rates of the bound ground-state YbLi⁺ molecules.

ACKNOWLEDGMENTS

M.G. acknowledges financial support from The Ulam Programme – Seal of Excellence grant of the Polish National Agency for Academic Exchange, Poland (Grant No. BPN/SEL/2021/1/00005/U/00001). P.T. acknowledges financial support from the OPUS research grant from the National Science Centre, Poland (Grant No. 2019/33/B/ST4/02114). We acknowledge that the results of this research have been achieved using the DECI resource Bem (Grant No. 412) based in Poland at Wrocław Centre for Networking and Supercomputing (WCSS, <http://wcss.pl>) with support from the PRACE aisbl. Funded/Co-funded by the European Union (ERC, DRESSED-pCCD, 101077420). Views and opinions expressed are, however, those of the author(s) only and do not necessarily reflect those of the European Union or

the European Research Council. Neither the European Union nor the granting authority can be held responsible for them.

- ¹E. S. Shuman, J. F. Barry, and D. DeMille, “Laser cooling of a diatomic molecule,” *Nature* **467**, 820–823 (2010).
- ²N. R. Hutzler, H.-I. Lu, and J. M. Doyle, “The buffer gas beam: An intense, cold, and slow source for atoms and molecules,” *Chem. Rev.* **112**, 4803–4827 (2012).
- ³J. Ulmanis, J. Deiglmayr, M. Repp, R. Wester, and M. Weidemüller, “Ultracold molecules formed by photoassociation: heteronuclear dimers, inelastic collisions, and interactions with ultrashort laser pulses,” *Chem. Rev.* **112**, 4890–4927 (2012).
- ⁴D. M. Bauer, M. Lettner, C. Vo, G. Rempe, and S. Dürr, “Control of a magnetic Feshbach resonance with laser light,” *Mol. Phys.* **5**, 339–342 (2009).
- ⁵R. J. Bartlett and M. Musiał, “Coupled-cluster theory in quantum chemistry,” *Rev. Mod. Phys.* **79**, 291–350 (2007).
- ⁶D. I. Lyakh, M. Musiał, V. F. Lotrich, and J. Bartlett, “Multireference nature of chemistry: The coupled-cluster view,” *Chem. Rev.* **112**, 182–243 (2012).
- ⁷H. Lischka, D. Nachtigallová, A. J. Aquino, P. G. Szalay, F. Plasser, F. B. Machado, and M. Barbatti, “Multireference approaches for excited states of molecules,” *Chem. Rev.* **118**, 7293–7361 (2018).
- ⁸M. B. Kosicki, D. Kędziera, and P. S. Żuchowski, “Ab initio study of chemical reactions of cold SrF and CaF molecules with alkali-metal and alkaline-earth-metal atoms: The implications for sympathetic cooling,” *J. Phys. Chem. A* **121**, 4152–4159 (2017).
- ⁹G. Visentin, A. A. Buchachenko, and P. Tecmer, “Reexamination of the ground-state Born-Oppenheimer Yb₂ potential,” *Phys. Rev. A* **104**, 052807 (2021).
- ¹⁰M. Borkowski, P. S. Żuchowski, R. Ciuryło, P. S. Julienne, D. Kędziera, Ł. Mentel, P. Tecmer, F. Münchow, C. Bruni, and A. Görlitz, “Scattering lengths in isotopologues of the RbYb system,” *Phys. Rev. A* **88**, 052708 (2013).
- ¹¹D. Kędziera, Ł. Mentel, P. S. Żuchowski, and S. Knoop, “Ab initio interaction potentials and scattering lengths for ultracold mixtures of metastable helium and alkali-metal atoms,” *Phys. Rev. A* **91**, 062711 (2015).
- ¹²M. Tomza, C. P. Koch, and R. Moszynski, “Cold interactions between an Yb⁺ ion and a Li atom: Prospects for sympathetic cooling, radiative association, and feshbach resonances,” *Phys. Rev. A* **91**, 042706 (2015).
- ¹³L. K. Sørensen, S. Knecht, T. Fleig, and C. M. Marian, “Four-component relativistic coupled cluster and configuration interaction calculations on the ground and excited states of the RbYb molecule,” *J. Phys. Chem. A* **113**, 12607–12614 (2009).
- ¹⁴S. N. Tohme, M. Korek, and R. Awad, “Ab initio calculations of the electronic structure of the low-lying states for the ultracold LiYb molecule,” *J. Chem. Phys.* **142** (2015).
- ¹⁵P. Tecmer, K. Boguslawski, M. Borkowski, P. S. Żuchowski, and D. Kędziera, “Modeling the electronic structures of the ground and excited states of the ytterbium atom and the ytterbium dimer: A modern quantum chemistry perspective,” *Int. J. Quantum Chem.* **119**, e25983 (2019).
- ¹⁶J. V. Pototschnig, K. G. Dyall, L. Visscher, and A. S. P. Gomes, “Electronic spectra of ytterbium fluoride from relativistic electronic structure calculations,” *Phys. Chem. Chem. Phys.* **23**, 22330–22343 (2021).
- ¹⁷A. Klein, Y. Shagam, W. Skomorowski, P. S. Żuchowski, M. Pawlak, L. M. Janssen, N. Moiseyev, S. Y. van de Meerakker, A. van der Avoird, C. P. Koch, *et al.*, “Directly probing anisotropy in atom–molecule collisions through quantum scattering resonances,” *Nucl. Phys.* **113**, 35–38 (2017).
- ¹⁸M. Tomza, K. Jachymski, R. Gerritsma, A. Negretti, T. Calarco, Z. Idziaszek, and P. S. Julienne, “Cold hybrid ion-atom systems,” *Rev. Mod. Phys.* **91**, 035001 (2019).
- ¹⁹M. Dolg, H. Stoll, and H. Preuss, “Ab initio pseudopotential study of YbH and YbF,” *Chem. Phys.* **165**, 21–30 (1992).

- ²⁰T. Su, C.-L. Yang, X.-Q. Wang, F.-J. Bai, and M.-S. Wang, "Theoretical characters of the ground states of YbX (X= F, Cl, Br, I, At)," *Chem. Phys. Lett.* **467**, 265–269 (2009).
- ²¹B. Roos, P. Taylor, and P. Siegbahn, "A complete active space SCF method-(CASSCF) using a density matrix formulated super-CI approach," *Chem. Phys.* **48**, 157–173 (1980).
- ²²S. N. Tohme and M. Korek, "Electronic structure with vibration-rotation study of the NaYb molecule," *Chem. Phys. Lett.* **638**, 216–226 (2015).
- ²³S. N. Tohme and M. Korek, "Electronic structure calculation of the KYb molecule with dipole moments, polarizabilities, and rovibrational studies," *Comput. Theory Chem.* **1078**, 65–71 (2016).
- ²⁴Q. Lu and K. A. Peterson, "Correlation consistent basis sets for lanthanides: The atoms La–Lu," *J. Chem. Phys.* **145** (2016).
- ²⁵X. Cao and M. Dolg, "Theoretical prediction of the second to fourth actinide ionization potentials," *Mol. Phys.* **101**, 961–969 (2003).
- ²⁶L. Visscher, "Approximate molecular relativistic Dirac-Coulomb calculations using a simple Coulombic correction," *Theor. Chem. Acc.* **98**, 68 (1997).
- ²⁷T. Saue, R. Bast, A. S. P. Gomes, H. J. A. Jensen, L. Visscher, I. A. Aucar, R. Di Remigio, K. G. Dyall, E. Eliav, E. Fasshauer, *et al.*, "The DIRAC code for relativistic molecular calculations," *J. Chem. Phys.* **152** (2020).
- ²⁸K. G. Dyall, "Relativistic double-zeta, triple-zeta, and quadruple-zeta basis sets for the light elements h–ar," *Theor. Chem. Acc.* **135**, 128 (2016).
- ²⁹A. S. Gomes, K. G. Dyall, and L. Visscher, "Relativistic double-zeta, triple-zeta, and quadruple-zeta basis sets for the lanthanides La–Lu," *Theor. Chem. Acc.* **127**, 369–381 (2010).
- ³⁰L. Visscher, K. G. Dyall, and T. J. Lee, "Kramers-restricted closed-shell CCSD theory," *Int. J. Quantum Chem.* **56**, 411–419 (1995).
- ³¹L. Visscher, T. J. Lee, and K. G. Dyall, "Formulation and implementation of a relativistic unrestricted coupled-cluster method including noniterative connected triples," *J. Chem. Phys.* **105**, 8769–8776 (1996).
- ³²A. Shee, T. Saue, L. Visscher, and A. Severo Pereira Gomes, "Equation-of-motion coupled-cluster theory based on the 4-component Dirac-Coulomb (–Gaunt) Hamiltonian. Energies for single electron detachment, attachment, and electronically excited states," *J. Chem. Phys.* **149** (2018).
- ³³K. G. Dyall, "An exact separation of the spin-free and spin-dependent terms of the dirac-coulomb-breit hamiltonian," *J. Chem. Phys.* **100**, 2118–2127 (1994).
- ³⁴P. J. Knowles and H.-J. Werner, "Internally contracted multiconfiguration-reference configuration interaction calculations for excited states," *Theor. Chim. Acta* **84**, 95–103 (1992).
- ³⁵E. R. Davidson, "Configuration interaction description of electron correlation," in *The World of Quantum Chemistry*, edited by R. Daudel and B. Pullman (Springer Netherlands, Dordrecht, 1974) pp. 17–30.
- ³⁶H.-J. Werner, P. J. Knowles, *et al.*, "Molpro, version 2020.2.1, a package of *ab initio* programs," (2020), see <http://www.molpro.net>.
- ³⁷H.-J. Werner, P. J. Knowles, G. Knizia, F. R. Manby, and M. Schütz, "Molpro: A General Purpose Quantum Chemistry Program Package," *WIREs Comput. Mol. Sci.* **2**, 242–253 (2012).
- ³⁸M. Hanauer and A. Köhn, "Pilot applications of internally contracted multireference coupled cluster theory, and how to choose the cluster operator properly," *J. Chem. Phys.* **134** (2011).
- ³⁹M. Hanauer and A. Köhn, "Perturbative treatment of triple excitations in internally contracted multireference coupled cluster theory," *J. Chem. Phys.* **136** (2012).
- ⁴⁰B. P. Prascher, D. E. Woon, K. A. Peterson, T. H. Dunning Jr, and A. K. Wilson, "Gaussian basis sets for use in correlated molecular calculations. vii. valence, core-valence, and scalar relativistic basis sets for li, be, na, and mg," *Theor. Chem. Acc.* , 69–82 (2011).
- ⁴¹A. Wolf, M. Reiher, and B. A. Hess, "The generalized Douglas–Kroll transformation," *J. Chem. Phys.* **117**, 9215–9226 (2002).
- ⁴²A. Wolf, M. Reiher, and B. A. Hess, "The generalized douglas–kroll transformation," *J. Chem. Phys.* **117**, 9215–9226 (2002).
- ⁴³M. Reiher and A. Wolf, "Exact Decoupling of the Dirac Hamiltonian. I. General Theory," *J. Chem. Phys.* **121**, 2037–2047 (2004).
- ⁴⁴M. Reiher and A. Wolf, "Exact Decoupling of the Dirac Hamiltonian. II. The Generalized Douglas–Kroll–Hess Transformation up to Arbitrary Order," *J. Chem. Phys.* **121**, 10945–10956 (2004).
- ⁴⁵M. Reiher and A. Wolf, *Relativistic Quantum Chemistry. The Fundamental Theory of Molecular Science* (Wiley, 2009).
- ⁴⁶P. Tecmer, K. Boguslawski, and D. Kedziera, "Relativistic methods in computational quantum chemistry," *Handbook of computational chemistry* **2**, 885–926 (2017).
- ⁴⁷A. Berning, M. Schweizer, H.-J. Werner, P. J. Knowles, and P. Palmieri, "Spin-orbit matrix elements for internally contracted multireference configuration interaction wavefunctions," *Mol. Phys.* **98**, 1823–1833 (2000).
- ⁴⁸Y. A. Aoto, QuAC - Quantum Atomic Collisions, v.1.0 <https://github.com/YuriAoto/QuAC> (2024).
- ⁴⁹J. Dunham, "The energy levels of a rotating vibrator," *Phys. Rev.* **41**, 721 (1932).
- ⁵⁰B. H. Bransden and C. J. Joachain, *Physics of Atoms and Molecules; 2nd ed.* (Prentice-Hall, Harlow, 2003).
- ⁵¹R. J. L. Roy and R. B. Bernstein, "Shape resonances and rotationally predissociating levels: The atomic collision time-delay functions and quasibound level properties of H₂ (X¹Σ_g⁺)," *J. Chem. Phys.* **154**, 5114 (1971).
- ⁵²W. F. Meggers and J. L. Tech, "The First Spectrum of Ytterbium (Yb I)," *J. Res. Natl. Bur. Stand. (U.S.)* **83**, 13–70 (1978).
- ⁵³W. Meggers, "The Second Spectrum of Ytterbium (Yb II)," *J. Res. Natl. Bu.r Stand. A Phys Chem.* **71A**, 396–546 (1967).
- ⁵⁴E. R. D. J. III, "NIST Computational Chemistry Comparison and Benchmark Database NIST Standard Reference Database Number 101," (2022).
- ⁵⁵R. J. Le Roy and R. B. Bernstein, "Shape Resonances and Rotationally Predissociating Levels: The Atomic Collision Time-Delay Functions and Quasibound Level Properties of H₂(X¹Σ_g⁺)," *J. Chem. Phys.* **54**, 5114–5126 (1971).

